JOURNAL OF THE ROYAL SOCIETY Interface

rsif.royalsocietypublishing.org

Research

Cite this article: McNamara ME, Saranathan V, Locatelli ER, Noh H, Briggs DEG, Orr PJ, Cao H. 2014 Cryptic iridescence in a fossil weevil generated by single diamond photonic crystals. *J. R. Soc. Interface* **11**: 20140736.
http://dx.doi.org/10.1098/rsif.2014.0736

Received: 7 July 2014
Accepted: 12 August 2014

Subject Areas:
biomaterials

Keywords:
fossil colour, structural colour, Coleoptera, iridescence, photonic crystals, photonic bandgap materials

Authors for correspondence:
Maria E. McNamara
e-mail: maria.mcnamara@ucc.ie
Vinod Saranathan
e-mail: vinodkumar.saranathan@aya.yale.edu

†Present address: School of Biological, Earth and Environmental Sciences, University College Cork, Cork, Ireland.
‡Present address: Division of Physics and Applied Physics, School of Physical and Mathematical Sciences, Nanyang Technological University, Singapore 637371, Singapore.

Electronic supplementary material is available at http://dx.doi.org/10.1098/rsif.2014.0736 or via http://rsif.royalsocietypublishing.org.

Royal Society Publishing

Cryptic iridescence in a fossil weevil generated by single diamond photonic crystals

Maria E. McNamara[1,2,†], Vinod Saranathan[3,‡], Emma R. Locatelli[1], Heeso Noh[4,5], Derek E. G. Briggs[1,6], Patrick J. Orr[2] and Hui Cao[5]

[1]Department of Geology and Geophysics, Kline Geology Laboratory, Yale University, 210 Whitney Avenue, New Haven, CT 06520, USA
[2]UCD School of Geological Sciences, University College Dublin, Belfield, Dublin 4, Ireland
[3]Edward Grey Institute, Department of Zoology, University of Oxford, Tinbergen Building, South Parks Road, Oxford OX1 3PS, UK
[4]Department of Nano and Electronic Physics, Kookmin University, 77 Jeong-neong Ro, Seongbuk-gu, Seoul, Korea
[5]Department of Applied Physics, Yale University, Becton Centre, 15 Prospect St., New Haven, CT 06520, USA
[6]Yale Peabody Museum of Natural History, 170 Whitney Avenue, New Haven, CT 06520, USA

Nature's most spectacular colours originate in integumentary tissue architectures that scatter light via nanoscale modulations of the refractive index. The most intricate biophotonic nanostructures are three-dimensional crystals with opal, single diamond or single gyroid lattices. Despite intense interest in their optical and structural properties, the evolution of such nanostructures is poorly understood, due in part to a lack of data from the fossil record. Here, we report preservation of single diamond (*Fd*-3*m*) three-dimensional photonic crystals in scales of a 735 000 year old specimen of the brown Nearctic weevil *Hypera diversipunctata* from Gold Run, Canada, and in extant conspecifics. The preserved red to green structural colours exhibit near-field brilliancy yet are inconspicuous from afar; they most likely had cryptic functions in substrate matching. The discovery of pristine fossil examples indicates that the fossil record is likely to yield further data on the evolution of three-dimensional photonic nanostructures and their biological functions.

1. Introduction

Colour is an essential component of visual displays in biological systems. Many organisms have evolved integumentary tissue nanostructures with periodic or quasi-periodic variations in the refractive index that interact with visible light (300–800 nm), scattering specific wavelengths preferentially to produce striking optical effects [1–5]. These biological photonic nanostructures produce structural colours that play important roles in sexual display and predator avoidance [6–8] and are especially diverse in insects [9] where one-, two- or three-dimensional biophotonic arrays have evolved. The most elaborate of these biophotonic nanostructures are three-dimensional lattices comprising opal, single diamond, single gyroid or quasi-ordered networks of chitin and air in the epicuticular scales of Lepidoptera (butterflies and moths) [2,10,11] and Coleoptera (beetles; see electronic supplementary material, table S1) [12]. Research on such three-dimensional biophotonic crystals (3DPCs) has focused on their optical properties [10–17] and potential for generating novel photonic devices [18,19]. Key aspects of the biology of these colour-producing structures, especially their evolutionary history and specific functions, however, remain poorly understood. Quasi-ordered or amorphous nanostructures are considered evolutionarily primitive relative to ordered lattices such as single diamonds [12]. This hypothesis has proved difficult to test, in part, because little is known about the fossilization potential of many relevant structures. In extant insects, 3DPCs are associated with diverse matte to strongly iridescent visual effects, but few studies [11,12,16] have investigated their biological functions

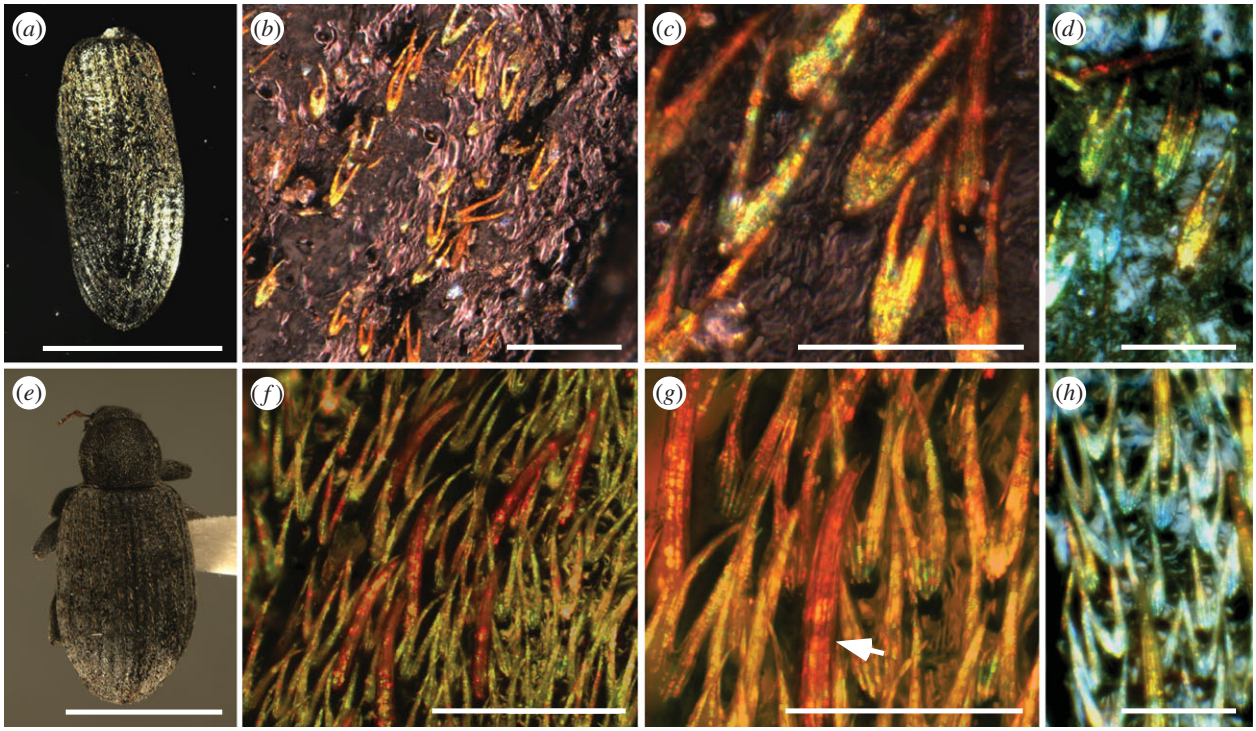

Figure 1. Structurally coloured scales from fossil (*a–d*) and modern (*e–h*) *Hypera diversipunctata*. (*a*,*e*) Light micrographs of the fossil specimen (an isolated elytron) (*a*) and of a complete modern specimen (*e*). (*b–d*, *f–h*) Light micrographs of fossil (*b–d*) and modern (*f–h*) scales showing bifurcate morphology and domains of different hues. Arrow in (*g*) indicates seta with multi-hued domains. Images in (*d*) and (*h*) were obtained under identical lighting conditions. Scale bars, (*a*,*e*) 2 mm; (*b*,*d*) 50 µm; (*c*,*f–h*) 25 µm. (Online version in colour.)

in detail. Fossil evidence has illuminated the functional evolution of other photonic nanostructures, for example multi-layer reflectors [20], but 3DPCs have not been described from the fossil record [21].

Here, we report the discovery of three-dimensional photonic crystals in a 735 000 year old fossil weevil from Yukon Territory, Canada. Intriguingly, the iridescent colours of these weevils are highly inconspicuous at long range despite their near-field brilliancy (figure 1). We used small-angle X-ray scattering (SAXS), scanning (SEM) and transmission electron microscopy (TEM) and reflectance spectrophotometry to identify the photonic nanostructure in the fossil weevil and in extant members of the same genus to assess the fidelity of preservation of the fossil. Our investigation confirms the potential of the fossil record and of extant taxa from tundra habitats to illuminate the evolutionary history of three-dimensional photonic nanostructures.

2. Material and methods

2.1. Fossil and modern specimens

The fossil weevil DG-B5 is held by the Department of Earth and Atmospheric Sciences at the University of Alberta, Edmonton, Canada. The specimen was recovered from a glacial diamict with a sandy silt matrix 200 mm above the Gold Run tephra at the former gold mine Gold Run in the Klondike gold field, Yukon, Canada (63.691° N, 138.6° W). Glass-isothermal plateau fission track dating indicates that the Gold Run tephra is 735 ± 88 ka [22]. Macrofossil plant and insect remains indicate a shrub–tundra palaeohabitat dominated by dwarf birch and willow [22]. Sediment samples were sieved using a screen box, sun-dried for several hours and transferred to plastic bags for further drying in the laboratory; macrofossil remains were picked by hand. The specimen was identified as *Hypera diversipunctata* by S. Kuzmina (University of Alberta) on the basis of the morphology of the elytron and the presence of strongly bifurcate scales. The modern specimen of *H. diversipunctata* (USNMNH 2060585) was collected in Yukon-Koyukuk County, Alaska, USA, and is held by the Smithsonian Institution National Museum of Natural History, Washington, DC.

2.2. Imaging

Light micrographs were obtained using a Leica DM2500P, a Leica VZ700C and a Zeiss Axioskop 2 microscope. Samples of elytron were prepared for electron microscopy as described in [23] and examined using a FEI XL-30 ESEM–FEG SEM at an accelerating voltage of 15 kV and a Zeiss EM900 TEM at 80 kV with an objective aperture of 90 nm diameter.

2.3. Focused ion beam milling

Scales from the fossil weevil were sputter-coated with Au and analysed using an FEI quanta dual-beam instrument. Selected areas were coated with Pt using a gas injection system and then milled using Ga ions at an accelerating voltage of 30 kV, a beam current of 0.4 pA and a pixel dwell time of 100 ns.

2.4. Microspectrophotometry

Reflectance spectra from cuticles were collected from a 70 or 500 µm diameter spot using an epi-illumination Nikon Optiphot 66 microscope and an Ocean Optics HR2000 + spectrophotometer, and calibrated using a matte white reflectance standard. Reflectance spectra from five natural sand samples (three from the Blackwater Estuary, Co. Cork, Ireland; two from Fermoyle, Co. Kerry, Ireland) were collected from a 2 mm diameter spot and calibrated as above.

2.5. Small-angle X-ray scattering

Small-angle X-ray scattering (SAXS) analyses were collected at beamline 8-ID-I of the Advanced Photon Source at Argonne

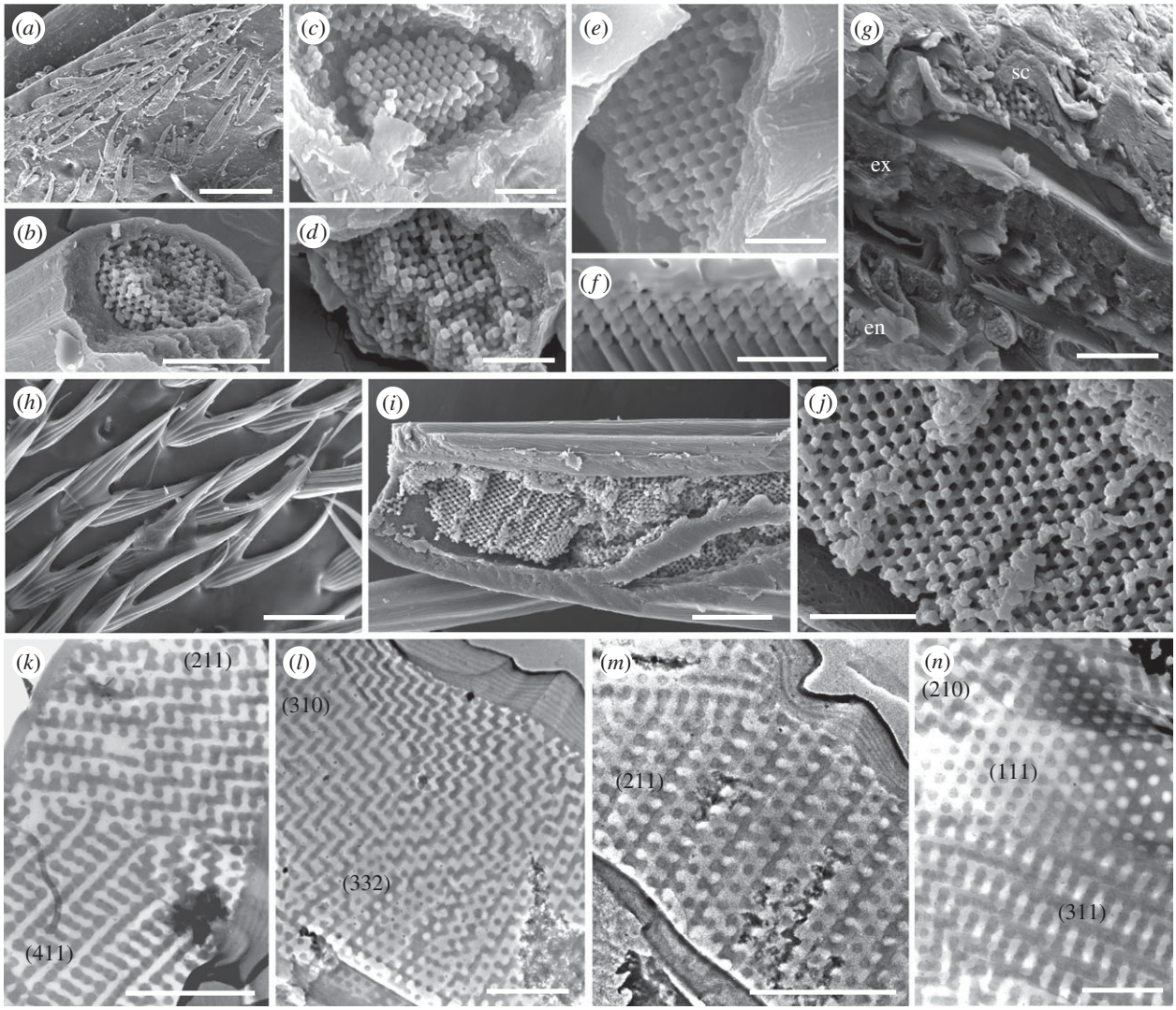

Figure 2. Electron micrographs of fossil (*a–g,k,l*) and modern (*h–j,m,n*) scales. (*k–n*) are transmission electron micrographs; all other images are scanning electron micrographs. (*a,h*) Surface of the fossil cuticle showing alignment of scales. (*b–f,i,j*) Detail of fractured scales showing 3DPCs in the scale lumen; (*f*) is an ion milled vertical section. (*g*) Fractured section through the cuticle of the fossil weevil showing fine lamination in the exocuticle (ex) and bundles of chitin microfibrils in the endocuticle (en); sc, scale. (*k–n*) Transmission electron micrographs of vertical sections of fossil (*k,l*) and modern (*m,n*) scales showing photonic polycrystallite domains. Numbers in parentheses denote distinctive motifs characteristic of specific planes of the single diamond morphology. Scale bars, (*a*) 50 μm; (*b*) 10 μm; (*c–f,k–n*) 1 μm; (*g,i*) 5 μm; (*h*) 25 μm; (*j*) 2 μm.

National Labs, Chicago, IL, USA. Pinhole SAXS data (15 μm horizontal × 15 μm vertical, 7.34 keV beam, 50 × 0.5 s exposures, sample to detector distance 4 m) were collected from individual weevil scales in transmission geometry and indexed as per standard protocol [10].

3. Results

The fossil specimen comprises an isolated elytron of the weevil *H. diversipunctata* (Curculionidae: *Subfamilia incertae sedis*: Hyperini). Both its cuticle and that of extant *H. diversipunctata* are a dull brown colour in hand specimen with no patterning apparent (figure 1*a,e*). Light microscopy revealed that the cuticle of the fossil and modern specimens is covered by hundreds of flattened bifurcate scales, each 45–55 μm long, 15–20 μm wide and 2–4 μm thick (figure 1*b–d,f–h*). Single scales are strongly iridescent and exhibit 5–25 microdomains that show red, yellow and green hues; those of the fossil scales are more saturated (figure 1*b–d,f–h*). Setae interspersed among the scales also exhibit coloured microdomains in the fossil (see electronic supplementary material, figure S1*a*) and modern (figure 1*f*, arrow) specimens. Electron micrographs revealed that most iridescent scales in the fossil, and all scales in the modern specimen, comprise a thin (0.9–1.2 μm thick) laminated outer cortex that envelopes a three-dimensional-ordered nanoscale lattice of chitin and air in the scale lumen (figure 2). The cuticle of the fossil weevil exhibits fine lamination in the exocuticle and bundles of chitin microfibrils in the endocuticle, similar to well-preserved beetle cuticles from other fossil localities [21]. SEM-EDAX spectra for the cuticle and scales of the fossil weevil elytron reveal prominent peaks only for carbon and oxygen. The fossil is organically preserved: there are no peaks for calcium or other elements (e.g. Fe, Mg, Mn, Sr, Ba) that would indicate the carbon is from a carbonate mineral. TEM images of the scales show diagnostic motifs that are characteristic of specific planes of the single diamond space group, confirming the fourfold coordination of the underlying nanostructure (figure 2*k–n*).

The SAXS patterns of fossil and extant weevil scales exhibit a concentric series of discrete Bragg scattering peaks (or spots)

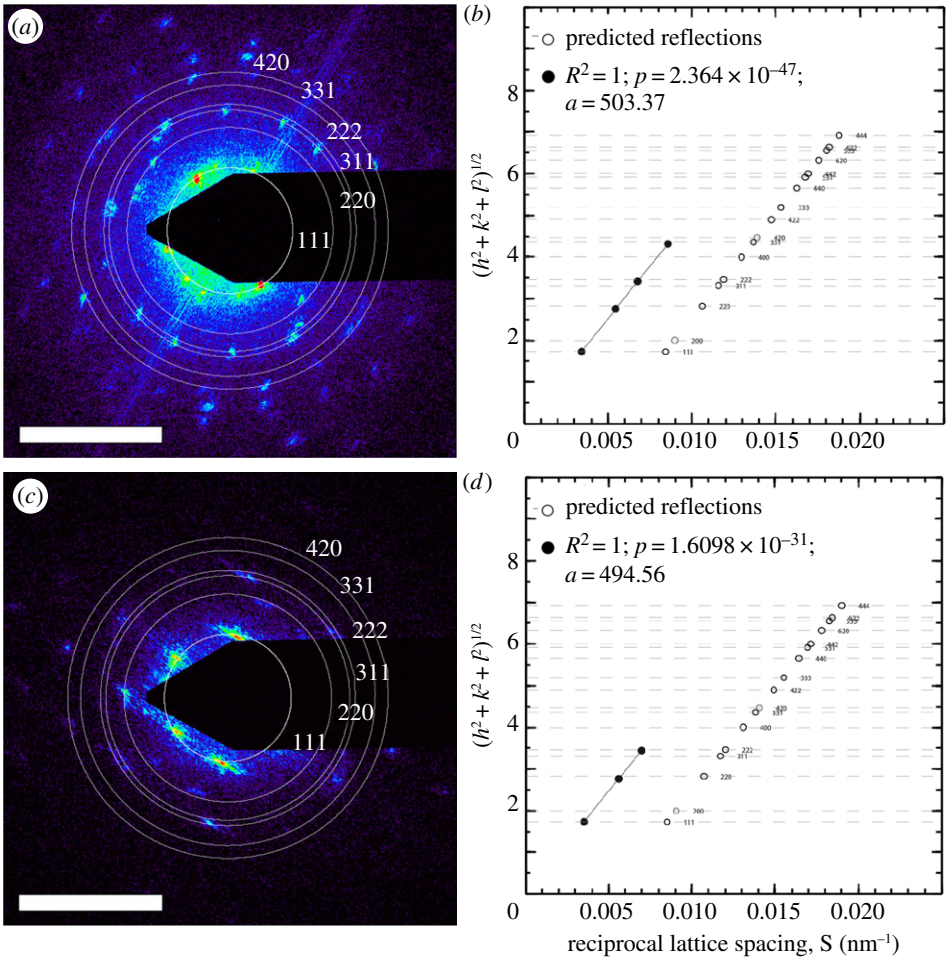

Figure 3. Two-dimensional small-angle X-ray scattering (SAXS) analyses of fossil and extant *H. diversipunctata* scales. (*a*,*c*) Unmasked SAXS patterns (original images 1340 × 1300 pixels) of fossil (*a*) and modern (*c*) scale. The false colour scale corresponds to the logarithm of scattering intensity. The concentric white circles denote the expected locations of the scattering peaks for the single diamond (*Fd*-3*m*) nanostructures. Scale bars, 0.05 nm. (*b*,*d*) Indexing the peaks of the azimuthally averaged profiles of the respective two-dimensional SAXS patterns in (*a*) and (*c*) and in electronic supplementary material figure S2, using the plot of the moduli of the *hkl* Miller indices of the Bragg peaks against the corresponding reciprocal lattice spacing S. The observed peaks (solid black circles) are shown alongside the theoretically allowed reflections for the single diamond (*Fd*-3*m*) and f.c.c. (*F4*-3*m*; in light grey) crystallographic space group symmetries. The linearity and zero intercepts of the plot confirm the cubic aspect of the nanostructures, and the slope gives an estimate of the lattice parameter. (Online version in colour.)

indicative of long-range crystal-like order [10] (figure 3*a*,*c* and see electronic supplementary material, figure S2). The irregular angles and spacings between the Bragg spots are consistent with the presence of many randomly oriented crystallite domains within the illuminated sample volume (figure 2*g*,*k* and see electronic supplementary material, figure S2). The azimuthally integrated scattering intensity profiles of the SAXS patterns feature at least two of the following discrete Bragg peaks with scattering wavevector positional ratios (q/q_{pk}): $\sqrt{3}$, $\sqrt{8}$, $\sqrt{11}$, $\sqrt{12}$ and $\sqrt{19}$ (figure 4 and see electronic supplementary material, S3). These peaks were indexed as reflections from (111), (220), (311), (222) and (331) planes, most consistent with the single diamond (space group no. 227, *Fd*-3*m*) crystallographic space group symmetry [24] (figure 4). The linearity and zero intercepts of the plots of reciprocal lattice spacings (S) versus the moduli of the assigned Miller indices (figure 3*b*,*d*) also confirm the cubic nature of the nanostructure. The slope of these *hkl* plots yields estimated lattice parameters [10] of 500.68 ± 6.59 and 521.63 ± 14.48 nm for the fossil and modern scales, respectively (see electronic supplementary material, figure S2 and table S2). The coherence length of the weevil scale nanostructures (a measure of the crystallite domain size) calculated from the full widths at half-maximum of the first-order SAXS peaks, $\xi \approx 2\pi/\Delta q$, is consistent with crystallite sizes observed in electron micrographs (figure 2*c*–*g*,*j*–*k* and see electronic supplementary material, table S2) [25].

Using the SAXS structural data, we predicted the optical reflectance spectra of the single diamond nanostructures in fossil and extant weevil scales with single scattering theory [10,26] (figure 5). The measured reflectances have peaks in the far-red to near-infrared region, consistent with the larger lattice constants (more than 500 nm) from SAXS structural measurements (see electronic supplementary material, table S2). Moreover, these lattice constants are comparable to those reported for other red iridescent weevil scales containing single diamond nanostructures [27]. The measured and predicted optical reflectance peaks agree reasonably well at higher wavelengths. However, the broader widths of the measured reflectance peak when compared with the optical prediction, especially at lower wavelengths, is likely because of multiple scattering of light, as in other 3DPCs [10]. The broadening of the peak is likely due to reflections (at lower wavelengths) from higher-order crystal planes of the single diamond photonic crystal as well as the strong interactions of coherently scattered light with the inherent disorder of the nanostructure [10,26,28,29]. Broad-field reflectance measurements for larger (500 µm) regions of cuticle

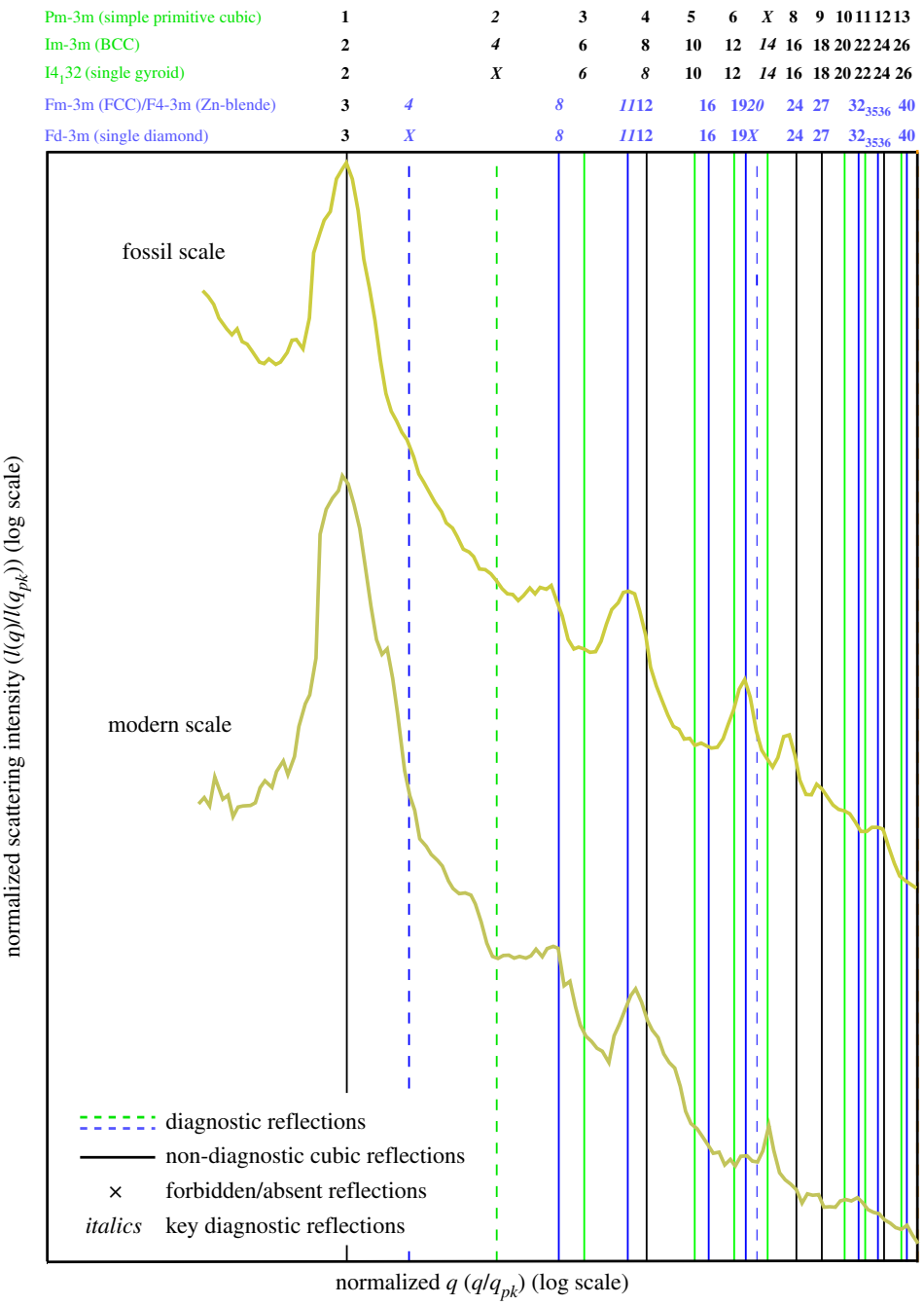

Figure 4. Structural diagnoses of normalized, azimuthally averaged SAXS profiles integrated from the respective two-dimensional SAXS patterns of photonic scales in figure 2. Vertical lines denote expected Bragg peak positional ratios for various cubic crystallographic space groups. Numbers above the vertical lines are squares of the moduli of the Miller indices (*hkl*) for the allowed reflections of the cubic space-groups. The normalized positional ratios of the scattering peaks are indexed to the predictions of specific crystallographic space-groups or symmetries following IUCr conventions [24]. (Online version in colour.)

lack a clear peak and appear relatively flat and unsaturated, albeit with progressively higher reflectance towards the longer-wavelength part of the visible spectrum (figure 5). These spectra closely resemble reflectance spectra from the natural sand samples (figure 5 and see electronic supplementary material, figure S3). Optical and structural data for the fossil and extant weevil scales indicate average refractive index values of 1.25 and 1.37, respectively, corresponding to a respective chitin volume fraction of 0.44 and 0.65. This is consistent with the relatively deeper red colour of the fossil *Hypera* and suggests that variations in both the peak structural correlation and the filling fraction of the scale nanostructures could account for interspecific differences in structural coloration in beetles, as in birds [30].

4. Discussion

4.1. Preservation

The preservation of visible iridescence and 3DPCs in the fossil weevil DG-B5 is attributed, in part, to minimal burial: colour-producing nanostructures, including 3DPCs, are known to degrade during diagenesis owing to elevated temperatures [21]. The dominant factors that impacted the fossil specimen are thus transport to the site of deposition and tissue decay. Many scales on the fossil elytron are represented by only the pedicle, indicating fracturing and loss of the rest of the scale during transport (figure 1*b*). Laboratory decay experiments have shown that tissue autolysis and microbial decay do not affect the physical structure or

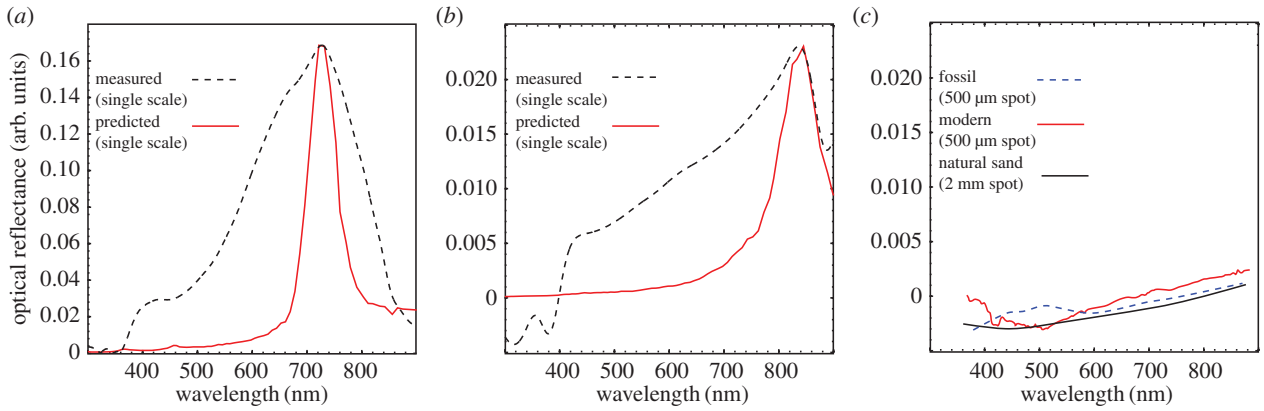

Figure 5. Measured optical reflectance spectra and single-scattering reflectance predictions from azimuthal average of SAXS patterns for single scales from fossil (*a*) and extant *H. diversipunctata* (*b*); (c) shows spectra from a 500 µm spot on the cuticle of fossil and extant specimens, and from a 2 mm spot of natural sand (Blackwater Estuary, Co. Waterford, Ireland). (Online version in colour.)

the colour produced by 3DPCs [21]. These data strongly indicate that the refractive index ($n = 1.56 + i0.06$ for chitin [31]) of the biophotonic nanostructure in the fossil weevil scales has not changed much during fossilization. The difference in hue between the fossil and modern weevils may reflect differences between subspecies or local variants.

4.2. Phylogenetic context

The discovery of single diamond photonic crystals in fossil and modern *H. diversipunctata* extends the known phylogenetic and temporal ranges of 3DPCs in nature and may shed light on the evolution of their structure and function. All known examples of 3DPCs in extant beetles are from one subfamily of longhorn beetles (Cerambycidae: Lamiinae) and one of weevils (Curculionidae: Entiminae; see electronic supplementary material, table S1) [12]. This phylogenetic distribution has been hypothesized to reflect the evolution of modified self-assembly mechanisms during scale development [10] in these, but not other, beetle groups [12]. Weevils and longhorn beetles share several attributes that have been identified as possible prerequisites for the evolution of 3DPCs. Each group includes diurnally active members that produce striking visual signals using modified, hollow scales and/or setae [12,32]. Single diamond photonic crystals have been identified only within weevils. The identification of these nanostructures in Hyperini has implications for weevil phylogeny, which has proved notoriously difficult to resolve [33–35]. The position of Hyperini within Curculioinidae is uncertain: the group may belong to the Curculioninae [36] or may form a clade that also includes Entiminae and other enigmatic tribes [34]. Discovery of 3DPCs in fossil and extant *Hypera* favours the latter scenario. It is also consistent with analysis of the phylogenetic distribution of 3DPCs in extant weevils that supports the grouping of Hyperini and Entiminae within a single clade, suggesting a single origin of 3DPCs within weevils [32] (V Saranathan & AE Seago 2013, unpublished data). Evolutionary scenarios for multi-layer reflectors and diffraction gratings involve multiple origination events in beetles, but these have not been elucidated at the subfamily level [12].

4.3. Function of the colour

The colours produced by photonic crystals in some lepidopterans [13,37] can confer evolutionary advantages by aiding mate recognition at close range. Such a signalling function has also been inferred for some weevils [16] and may operate even in taxa characterized by a diffuse long-range visual signal, provided specular highlights are visible to conspecifics at short range [16]. In *H. diversipunctata*, scales comprise multiple reflecting domains. Assuming a maximum domain size of 10 µm and an angular resolution of 1° [38], individual spots of colour cannot be distinguished at a distance of more than 0.575 mm. The iridescent colours are thus unlikely to function in sexual display or as warning coloration; other functions (e.g. thermoregulation, mechanical resistance, photoprotection) are not immediately obvious. The selective force driving the evolution of highly sophisticated biophotonic nanostructures within *H. diversipunctata* is therefore likely to have been crypsis. This is supported by the flat, unsaturated reflectance spectrum of the cuticle from a large diameter spot, and the close resemblance of this spectrum to those of the natural sand samples (figure 5 and see supplementary electronic material, figure S3). The fossil taxon *H. diversipunctata* inhabited a shrub–tundra palaeoenvironment [22] (see Material and methods). Its ecology is similar to that of extant *Hypera* species, which are xerophilic members of upland cryophytic steppe and tundra environments ranging from dry gravels to moderately moist scrub habitats [39,40].

Almost all other weevil taxa with well-characterized 3DPCs are from tropical and subtropical forest biotopes in South America, Africa and Asia (see electronic supplementary material, table S1) [12]. Such (sub)tropical habitats comprise closely juxtaposed regions of bright sunlight and shade. Extant entimine weevils and lamiine longhorn beetles with 3DPCs typically exhibit brilliant colours, striking colour patterns and/or strong iridescence effects in these environments, presumably employed in inter- and intraspecific signalling [12]. Green hues produced by 3DPCs in some weevils [12,16] and lepidopterans [8,10,11] are considered to function in crypsis, but 3DPCs can also be incorporated into striking colour patterns with possible aposematic functions [8,12].

The dark brown colour and cryptic iridescence of *H. diversipunctata* are probably adaptations to life on exposed soils, facilitating substrate matching to avoid predation. In other weevils [16] and in matte green papilionid and lycaenid butterflies [10,37], the distribution of photonic scales over the entire body surface and the highly polycrystalline nature of the photonic crystals create an angle-independent diffuse visual signal at long range. Similar diffuse colours used in substrate matching are achieved via additive colour mixing in

structurally coloured tiger beetles (Carabidae) [41], darkling beetles (Tenebrionidae) [42] and scarabs (Scarabaeidae) [43,44]. However, epicuticular scales with 3DPCs are not necessary to produce dark brown matte colours. Insect cuticle is typically brown to black and a matte effect is often achieved using diffuse pigmentation and modification of the cuticle surface [12].

4.4. Evolutionary implications

The early evolutionary history of 3DPCs in weevils has been associated with the production of cryptic visual signals [32]. Indeed, several basal members of Curculionidae bear quasi-ordered or amorphous single diamond biophotonic nanostructures within matte reddish-brown scales (V Saranathan & AE Seago 2013, unpublished data). Thus, quasi-ordered scattering arrays producing cryptic colours may have given rise to nanostructures with crystalline microdomains, such as in *H. diversipunctata*, and ultimately more complex ordered 3DPCs, with larger domains, capable of producing bright colours with diverse signalling functions [32]. Bright visual signals could be achieved by increasing the size of crystal domains and individual scales, and by organizing scales into high-density clusters or patches. Such modifications to 3DPC-bearing scales could have been achieved relatively easily as insect epidermal cells are known for their developmental plasticity [45,46]. In lepidopterans, three-dimensional photonic nanostructures are hypothesized to develop via intracellular self-assembly of plasma and smooth endoplasmic reticulum membrane systems [10,47]. Similar membrane self-assembly processes are likely to control development of 3DPCs in weevils [12] and may facilitate rapid evolution of complex photonic nanostructures without strong genetic control [48].

The fossil nanostructures described herein represent the first example, to the best of our knowledge, of 3DPCs in the fossil record, confirming, as predicted [21], that such nanostructures can be fossilized with a high degree of fidelity. This identifies the Pleistocene fossil record as a new and potentially extensive source of data on the evolution of 3DPCs. Further, we show that complex three-dimensional photonic nanoarchitectures occur in insects with an unremarkable matte coloration. As the existence of such nanostructures may not be apparent in hand specimens, it is likely that cryptic iridescence, and three-dimensional photonic nanostructures, are much more widespread in diverse visually non-descript extant insects than we realize. Indeed, our examination of other extant *Hypera* species reveals the presence of iridescent scales (see electronic supplementary material, figure S1*e*,*f*). Further investigation of other extant and fossil beetle taxa coupling genetic analysis and ultrastructural study of their cuticle will yield important information on the diversity of 3DPCs in nature and the respective roles of visual function and developmental processes in driving their evolution.

Data accessibility. All data from reflectance spectrophotometry and SAXS analyses are available at the Cork Open Research Archive (CORA) (http://cora.ucc.ie). Requests for specimens and samples should be addressed to M.E.M.

Acknowledgements. We thank Svetlana Kuzmina for lending the fossil *Hypera*, David Furth at the Smithsonian Institution for lending modern *H. diversipunctata*, and Padraig Whelan and Britta Zeckel for lending the sediment samples. Zhenting Jiang and Stuart Kearns assisted with scanning electron microscopy, Barry Piekos with transmission electron microscopy, Michael Rooks with focused ion beam milling, Alec Sandy and Suresh Narayan with SAXS, and Hugh Doyle with microspectrophotometry. Scott Elias, Duane Froese and Rick Prum provided useful discussion. SAXS analyses were supported by the US Department of Energy, Office of Science, Office of Basic Energy Sciences, under contract DE-AC02-06CH11357.

Funding statement. The research was supported by an IRCSET-Marie Curie International Mobility Fellowship and Tyndall National Institute NAP 434 grant awarded to M.E.M. and by a UK Royal Society Newton Fellowship and a Linacre College EPA Cephalosporin Junior Research Fellowship awarded to V.S.

References

1. Vukusic P, Sambles JR. 2003 Photonic structures in biology. *Nature* **424**, 852–855. (doi:10.1038/nature01941)
2. Prum RO, Quinn T, Torres RH. 2006 Anatomically diverse butterfly scales all produce structural colors by coherent scattering. *J. Exp. Biol.* **209**, 748–765. (doi:10.1242/jeb.02051)
3. Kinoshita S, Yoshioka S. 2005 *Structural colors in biological systems: principles and applications*, p. 351. Osaka, Japan: Osaka University Press.
4. Parker AR. 1999 Invertebrate structural colours. In *Functional morphology of the invertebrate skeleton* (ed. E Savazzi), pp. 65–90. London, UK: Wiley.
5. Srinivasarao M. 1999 Nano-optics in the biological world: beetles, butterflies, birds, and moths. *Chem. Rev.* **99**, 1935–1961. (doi:10.1021/cr970080y)
6. Sweeney A, Jiggins C, Johnsen S. 2003 Polarized light as a butterfly mating signal. *Nature* **423**, 31–32. (doi:10.1038/423031a)
7. Doucet SM, Meadows MG. 2009 Iridescence: a functional perspective. *J. R. Soc. Interface* **6**, S115–S132. (doi:10.1098/rsif.2008.0395.focus)
8. Wilts BD, Michielsen K, De Raedt H, Stavenga DG. 2012 Iridescence and spectral filtering of the gyroid-type photonic crystals in *Parides sesostris* wing scales. *Interface Focus* **2**, 681–687. (doi:10.1098/rsfs.2011.0082)
9. Kinoshita S. 2008 *Structural colours in the realm of nature*, p. 368. Singapore: World Scientific.
10. Saranathan V, Osuji CO, Mochrie SGJ, Noh H, Narayanan S, Sandy A, Dufresne ER, Prum RO. 2010 Structure, function, and self-assembly of single network gyroid (I4132) photonic crystals in butterfly wing scales. *Proc. Natl Acad. Sci. USA* **107**, 11 676–11 681. (doi:10.1073/pnas.0909616107)
11. Michielsen K, Stavenga DG. 2008 Gyroid cuticular structures in butterfly wing scales: biological photonic crystals. *J. R. Soc. Interface* **5**, 85–94. (doi:10.1098/rsif.2007.1065)
12. Seago AE, Brady P, Vigneron J-P, Schultz TD. 2009 Gold bugs and beyond: a review of iridescence and structural colour mechanisms in beetles (Coleoptera). *J. R. Soc. Interface* **6**, S165–S184. (doi:10.1098/rsif.2008.0354.focus)
13. Poladian L, Wickham S, Lee K, Large MC. 2009 Iridescence from photonic crystals and its suppression in butterfly scales. *J. R. Soc. Interface* **6**, S233–S242. (doi:10.1098/rsif.2008.0353.focus)
14. Saba M, Thiel M, Turner MD, Hyde ST, Gu M, Grosse-Brauckmann K, Neshev DN, Mecke K, Schröder-Turk GE. 2011 Circular dichroism in biological photonic crystals and cubic chiral nets. *Phys. Rev. Lett.* **106**, 103–902. (doi:10.1103/PhysRevLett.106.103902)
15. Parker AR, Welch VL, Driver D, Martini N. 2003 Structural colour: opal analogue discovered in a weevil. *Nature* **426**, 786–787. (doi:10.1038/426786a)
16. Wilts BD, Michielsen K, Kuipers J, De Raedt H, Stavenga DG. 2012 Brilliant camouflage: photonic crystals in the diamond weevil, *Entimus imperialis*. *Proc. R. Soc. B* **279**, 2524–2530. (doi:10.1098/rspb.2011.2651)
17. Galusha JW, Richey LR, Gardner JS, Cha JN, Bartl MH. 2008 Discovery of a diamond-based photonic

crystal structure in beetle scales. *Phys. Rev. E.* **77**, 050904. (doi:10.1103/PhysRevE.77.050904)

18. Biró LP, Vigneron JP. 2011 Photonic nanoarchitectures in butterflies and beetles: valuable sources for bioinspiration. *Laser Photon. Rev.* **5**, 27–51. (doi:10.1002/lpor.200900018)
19. Parker AR, Townley HE. 2007 Biomimetics of photonic nanostructures. *Nat. Nanotechnol.* **2**, 347–353. (doi:10.1038/nnano.2007.152)
20. McNamara ME, Briggs DEG, Orr PJ, Wedmann S, Noh H, Cao H. 2011 Fossilized biophotonic nanostructures reveal the original colors of 47-million-year-old moths. *PLoS Biol.* **9**, e1001200. (doi:10.1371/journal.pbio.1001200)
21. McNamara ME *et al*. 2013 The fossil record of insect color illuminated by maturation experiments. *Geology* **47**, 487–490. (doi:10.1130/G33836.1)
22. Westgate JA *et al*. 2009 Gold Run tephra: a Middle Pleistocene stratigraphic and paleoenvironmental marker across west-central Yukon Territory, Canada. *Can. J. Earth Sci.* **46**, 465–478. (doi:10.1139/E09-029)
23. McNamara ME, Briggs DEG, Orr PJ, Noh H, Cao H. 2012 The original colours of fossil beetles. *Proc. R. Soc. B* **279**, 1114–1121. (doi:10.1098/rspb.2011.1677)
24. Hahn T. 2006 The 230 space groups. In *IUCr international tables for crystallography* (eds T Hahn, MI Aroyo), pp. 112–117. Berlin, Germany: Springer.
25. Förster S, Timmann A, Schellbach C, Frömsdorf A, Kornowski A, Weller H, Roth SV, Lindner P. 2007 Order causes secondary Bragg peaks in soft materials. *Nat. Mater.* **6**, 888–893. (doi:10.1038/nmat1995)
26. Noh H, Liew SF, Saranathan V, Prum RO, Mochrie SGl, Dufresne HC. 2010 How noniridescent colors are generated by quasi-ordered structures of bird feathers. *Adv. Mater.* **22**, 2871–2880. (doi:10.1002/adma.201090094)
27. Galusha JW, Richey LR, Jorgensen MR, Gardner JS, Bartl MH. 2010 Study of natural photonic crystals in beetle scales and their conversion into inorganic structures *via* a sol–gel bio-templating route. *J. Mater. Chem.* **20**, 1277–1284. (doi:10.1039/b913217a)
28. Noh H, Liew SF, Saranathan V, Prum RO, Mochrie SG, Dufresne E, Cao H. 2010 Contribution of double scattering to structural coloration in quasi-ordered nanostructures of bird feathers. *Phys. Rev. E* **81**, 051923. (doi:10.1103/PhysRevE.81.051923)
29. Liew SF *et al*. 2011 Short-range order and near-field effects on optical scattering and structural coloration. *Opt. Express.* **19**, 8208–8217. (doi:10.1364/OE.19.008208)
30. Saranathan V, Forster J, Noh H, Liew S, Mochrie S, Cao H, Dufresne E, Prum R. 2012 Structure and optical function of amorphous photonic nanostructures from acian feather barbs: a comparative small angle X-ray scattering (SAXS) analysis of 230 bird species. *J. R. Soc. Interface* **9**, 2563–2580. (doi:10.1098/rsif.2012.0191)
31. Vukusic P, Sambles JR, Lawrence CR, Wootton RJ. 1999 Quantified interference and diffraction in single Morpho butterfly scales. *Proc. R. Soc. Lond. B* **266**, 1403–1411. (doi:10.1098/rspb.1999.0794)
32. Seago AS, Saranathan V. 2012 Photonic crystals in beetles. In *Nature's nanostructures* (eds A Barnard, H Guo), pp. 313–329. Singapore: Pan Stanford Publishing.
33. Franz NM, Engel MS. 2010 Can higher-level phylogenies of weevils explain their evolutionary success? A critical review. *Syst. Entomol.* **35**, 597–606. (doi:10.1111/j.1365-3113.2010.00534.x)
34. McKenna D, Sequeira A, Marvaldi A, Farrell B. 2009 Temporal lags and overlap in the diversification of weevils and flowering plants. *Proc. Natl Acad. Sci. USA* **106**, 7083–7088. (doi:10.1073/pnas.0810618106)
35. Marvaldi AE, Sequeira AS, O'Brien CW, Farrell BD. 2002 Molecular and morphological phylogenetics of weevils (Coleoptera: Curculionoidea): do niche shifts accompany diversification? *Syst. Biol.* **51**, 761–785. (doi:10.1080/10635150290102465)
36. Oberprieler RG, Marvaldi AE, Anderson RS. 2008 Weevils, weevils, weevils everywhere. *Zootaxa* **1668**, 491–520.
37. Michielsen K, De Raedt H, Stavenga DG. 2010 Reflectivity of the gyroid biophotonic crystals in the ventral wing scales of the Green Hairstreak butterfly, *Callophrys rubi*. *J. R. Soc. Interface* **7**, 765–771. (doi:10.1098/rsif.2009.0352)
38. Land MF. 1997 Visual acuity in insects. *Annu. Rev. Entomol.* **42**, 147–177. (doi:10.1146/annurev.ento.42.1.147)
39. Anderson RS. 1997 Weevils (Coleoptera: Curculionoidea, excluding Scolytinae and Platypodinae) of the Yukon. In *Insects of the Yukon* (eds HV Danks, JA Downes), pp. 523–562. Ottawa, Canada: Biological Survey of Canada (Terrestrial Arthropods).
40. Khruleva OA, Korotyaev BA. 1999 Weevils (Coleoptera: Apionidae, Curculionidae) of Wrangel Island. *Entomol. Rev.* **78**, 648–670. [in Russian.]
41. Schultz TD. 1986 Role of structural colors in predator avoidance by tiger beetles of the genus *Cincindela* (Coleoptera: Cincindelidae). *Bull. Entomol. Soc. Am.* **32**, 142–146.
42. Liu F, Yin H, Dong B, Qing Y, Zhao L, Meyer S, Liu X, Zi J, Chen B. 2008 Inconspicuous structural coloration in the elytra of beetles *Chlorophila obscuripennis* (Coleoptera). *Phys. Rev. E.* **77**, 12901. (doi:10.1103/PhysRevE.77.012901)
43. Jewell SA, Vukusic P, Roberts NW. 2007 Circularly polarized colour reflection from helicoidal structures in the beetle *Plusiotis boucardi*. *New J. Phys.* **9**, 99. (doi:10.1088/1367-2630/9/4/099)
44. De Silva L, Hodgkinson I, Murray P, Wu QH, Arnold M. 2005 Natural and nanoengineered chiral reflectors: structural color of manuka beetles and titania coatings. *Electromagnetics* **25**, 391–408. (doi:10.1080/02726340590957399)
45. Ghiradella H. 1989 Structure and development of iridescent butterfly scales: lattices and laminae. *J. Morphol.* **202**, 69–88. (doi:10.1002/jmor.1052020106)
46. Carroll SB, Galant R, Skeath JB, Paddock S, Lewis DL. 1998 Expression pattern of a butterfly achaete-scute homolog reveals the homology of butterfly wing scales and insect sensory bristles. *Curr. Biol.* **8**, 807–813. (doi:10.1016/S0960-9822(98)70322-7)
47. Ghiradella H. 2010 Insect cuticular surface modifications: scales and other structural formations. *Adv. Insect Physiol.* **38**, 136–180. (doi:10.1016/S0065-2806(10)38006-4)
48. Ingram AL, Parker AR. 2008 A review of the diversity and evolution of photonic structures in butterflies, incorporating the work of John Huxley (The Natural History Museum, London from 1961 to 1990). *Phil. Trans. R. Soc. B* **363**, 2465–2480. (doi:10.1098/rstb.2007.2258)